

DreamDance: Animating Human Images by Enriching 3D Geometry Cues from 2D Poses

Yatian Pang^{1,3}, Bin Zhu¹, Bin Lin¹, Mingzhe Zheng⁴,
Francis E. H. Tay³, Ser-Nam Lim^{5,6}, Harry Yang^{4,6}, Li Yuan^{1,2,†}

¹ Peking University ² PengCheng Laboratory ³ NUS ⁴ HKUST ⁵ UCF ⁶ Everlyn AI

Abstract

In this work, we present **DreamDance**, a novel method for animating human images using only skeleton pose sequences as conditional inputs. Existing approaches struggle with generating coherent, high-quality content in an efficient and user-friendly manner. Concretely, baseline methods relying on only 2D pose guidance lack the cues of 3D information, leading to suboptimal results, while methods using 3D representation as guidance achieve higher quality but involve a cumbersome and time-intensive process. To address these limitations, **DreamDance** enriches 3D geometry cues from 2D poses by introducing an efficient diffusion model, enabling high-quality human image animation with various guidance. Our key insight is that human images naturally exhibit multiple levels of correlation, progressing from coarse skeleton poses to fine-grained geometry cues, and further from these geometry cues to explicit appearance details. Capturing such correlations could enrich the guidance signals, facilitating intra-frame coherency and inter-frame consistency. Specifically, we construct the *TikTokDance5K* dataset, comprising 5K high-quality dance videos with detailed frame annotations, including human pose, depth, and normal maps. Next, we introduce a *Mutually Aligned Geometry Diffusion Model* to generate fine-grained depth and normal maps for enriched guidance. Finally, a *Cross-domain Controller* incorporates multi-level guidance to animate human images effectively with a video diffusion model. Extensive experiments demonstrate that our method achieves state-of-the-art performance in animating human images. Webpage: <https://pang-yatian.github.io/Dreamdance-webpage/>

1. Introduction

Human image animation refers to generating dynamic and realistic videos from static human images following a sequence of motion control signals. This field has attracted significant academic interest due to its diverse applications

Guidance Type	2D Pose	2D DensePose	2D Pose + 3D SMPL	2D Pose + Normal, Depth
User-friendly	✓	✓	✗	✓
Rich Guidance	✗	✗	–	✓
Temporal Prior	✗	✗	✗	✓

Figure 1. A summarized comparison between DreamDance and the baseline methods.

across industries, including film production, social media, and online retail. Despite the rapid development of generative artificial intelligence, human image animation remains challenging because it requires a comprehensive understanding of both intra-frame coherency and inter-frame consistency.

Recently, diffusion models [25, 61] have demonstrated remarkable potential in image [6, 48, 53, 54] and video [4, 5, 83, 88, 95] generation, unlocking new possibilities for human image animation tasks. Pioneer works such as Disco [68] and Dreampose [36] leverage input images and pose conditions to generate target frames sequentially. However, due to the lack of temporal learning capabilities, these methods often suffer from flickering artifacts and temporal inconsistency across frames. To address these limitations, more recent methods such as MagicAnimate [79] and AnimateAnyone [29] incorporate temporal attention blocks into the diffusion network to enhance temporal coherence. Despite this improvement, their generation quality remains

constrained by coarse control conditions, leading to inconsistent and incoherent visual outputs. To further improve control precision, Champ [96] introduces a 3D parametric human model SMPL [42] to provide additional guidance. By first generating SMPL motions and then rendering them into normal and depth maps, this approach integrates geometric information with pose sequences for human image animation. However, SMPL-based methods present significant drawbacks. First, generating SMPL motions is cumbersome and not user-friendly, as it typically relies on predictions from existing videos, which limits editability and flexibility compared to the more intuitive manipulation of poses using open-source tools like the GUI [46]. Second, the independence between SMPL and pose models can lead to misalignment between control signals, resulting in imprecise adherence to the intended pose sequences. Additionally, SMPL’s rendering primarily emphasizes body geometry while neglecting crucial visual details, such as clothing and hair, which can contribute to temporal incoherence and visual inconsistencies. Furthermore, these methods take image diffusion models as base models, which lack a strong temporal prior, resulting in poor temporal consistency in the generated videos. We summarize existing methods in Figure 1.

To this end, we propose **DreamDance**, a unified framework for animating human images using only skeleton pose sequences as original guidance signals. Our key insight is the recognition of multi-level correlations inherent in human images, extending from coarse skeleton poses to fine-grained geometry cues, and further to explicit appearance details. Capturing these correlations could enrich the guidance signals, thereby enhancing both intra-frame coherence and inter-frame consistency in the animation process. To achieve this, we first construct a dataset, TikTok-Dance5K, comprising 5,000 high-quality dance videos, each annotated with human pose, depth, and normal maps for every frame. Building on this dataset, we propose a novel framework comprising two diffusion models. Specifically, the Mutually Aligned Geometry Diffusion Model generates detailed depth and normal maps to enrich the guidance signals. To ensure the robustness and effectiveness of the generated guidance signals, we introduce geometry attention and temporal attention modules, which align guidance across modality and temporal dimensions. With the enriched geometry cues, the Cross-Domain Controlled Video Diffusion Model utilizes a cross-domain controller to integrate multiple levels of guidance, animating human images with high quality. Besides, we implement a robust conditioning scheme to reduce the impact of error accumulation in our two-stage generation pipeline. Extensive experiments demonstrate that DreamDance achieves state-of-the-art performance in animating human images, significantly improving both visual coherence and temporal consistency

compared to existing methods. We again highlight the comparison in Figure 1 and show that by eliminating the need for complex and rigid 3D models, our approach provides greater flexibility, ease of use, and finer control over the animation process, establishing it as a highly effective solution for animating human images.

To sum up, this work contributes in the following ways:

- We construct the TikTok-Dance5K dataset, comprising 5,000 high-quality human dance videos with comprehensive visual annotations. It will be made publicly available to support further research in the field.
- We propose the Mutually Aligned Geometry Diffusion model, which generates detailed depth and normal maps to enrich guidance signals. To ensure robustness, we incorporate geometry and temporal attention modules that align geometric information across modality and temporal dimensions.
- We introduce the Cross-Domain Controlled Video Diffusion Model, which utilizes a cross-domain controller to integrate multiple levels of guidance for high-quality human image animating. A robust conditioning scheme further mitigates the effects of error accumulation in our two-stage generation pipeline.
- Our extensive experiments demonstrate that our framework achieves state-of-the-art performance in animating human images, setting a new benchmark for visual coherence and temporal consistency compared to existing methods.

2. Related Works

2.1. Diffusion Models for Image Generation

Diffusion models have achieved significant success in generating images given various conditions. Notably, Stable Diffusion [53] has demonstrated its potential in producing high-quality images from text prompts as the conditioning input. To introduce additional control over the generation process, ControlNet [92] proposes training an additional copy of the pre-trained diffusion model to incorporate extra control signals, such as pose, depth, and canny edges. Subsequently, many works [45, 57, 84] propose incorporating more complex control signals for enhanced controllability in image generation. In this work, we focus on using pose as the control signal and propose generating fine-grained depth and normal maps to provide supplementary guidance. Several works [41, 47, 51] propose generating geometry maps with diffusion models to improve the quality of the generated 3D geometry. Other works [16, 37] propose to utilize diffusion models for depth and normal estimation tasks. To generate precise human images, Hyperhuman [40] proposes a latent structural diffusion model to jointly capture the human image appearance and geometry relationship. Their diffusion model consists of different expert branches and

only supports text as input conditions. In our work, we propose a novel geometry diffusion model by introducing a geometry attention mechanism and utilizing a reference net for fine-grained reference image control. We also incorporate temporal attention to enable the geometric generation along the temporal dimension.

2.2. Diffusion Models for Video Generation

The great potential of diffusion models in image generation has inspired extensive research in applying them to video generation and other domains. [10, 11, 13, 18, 20, 30, 34, 35, 38, 47, 49, 50, 56, 62, 72, 75, 85, 87, 90, 91, 97]. Pioneer works [13, 26, 27, 38, 59] focus on extending image-based diffusion models using temporal modules to address the dynamics of video sequences and generating videos. Video LDM [5] first pre-train the model on images and then fine-tune it on video data by incorporating temporal layers. Animatediff [21] add additional motion modules into pre-trained text-to-image diffusion models and train them with video data. Stable Video Diffusion (SVD) [4] is a latent video diffusion model for high-resolution image-to-video generation. The authors identify and evaluate three different stages for successful training of the video diffusion model and explore a unified strategy for curating video data. In this work, we construct SVD-ControlNet and take Stable Video Diffusion as the base model because it possesses a strong temporal prior and temporal consistency compared to training from scratch or adapting from image diffusion models.

2.3. Diffusion Models for Human Image Animation

Human image animation aims to generate dynamic and realistic human motion videos given a static human image and a sequence of control signals [1, 7, 8, 14, 15, 17, 19, 22, 23, 31, 33, 39, 43, 44, 52, 55, 63, 64, 66, 67, 69–71, 74, 76–78, 80, 86, 89, 94]. Recent works utilize the successful diffusion models for this task. DreamPose [36] and DISCO [68] modify the diffusion model to integrate the information from the reference image and control signal. However, they animate the human image in a frame-by-frame manner, which lacks temporal consistency. The following works AnimateAnyone [29], MagicAnimate [79], and MagicPose [9] propose a similar framework that uses a reference network for human feature injection and also utilizes motion modules to enhance temporal consistency. The recent work Champ [96] introduces the use of a 3D parametric human model, SMPL, to provide additional conditions for human image animation by generating normal and depth maps from SMPL motions. However, this approach has limitations, including the complexity of creating SMPL motions, potential misalignment between SMPL and pose models, and the omission of important details like outfits and hair, leading to less coherent generated content. Our

method addresses these limitations by proposing a Mutually Aligned Geometry Diffusion Model to jointly capture human image appearance and geometry relationship, achieving efficiency and high quality.

3. Preliminaries and Problem Formulation

3.1. Diffusion Models

Diffusion models, as introduced in previous works [25, 60], aim to approximate a data distribution $q(\mathbf{x})$ by learning a probabilistic model $p_\theta(\mathbf{x}_0) = \int p_\theta(\mathbf{x}_{0:T}) d\mathbf{x}_{1:T}$. The joint distribution between \mathbf{x}_0 and random latent variables $\mathbf{x}_{1:T}$ is defined through a reverse Markov Chain, $p_\theta(\mathbf{x}_{0:T}) = p(\mathbf{x}_T) \prod_{t=1}^T p_\theta(\mathbf{x}_{t-1}|\mathbf{x}_t)$, where $p(\mathbf{x}_T)$ is modeled as a standard normal distribution, and the transition kernels are expressed as $p_\theta(\mathbf{x}_{t-1}|\mathbf{x}_t) = \mathcal{N}(\mathbf{x}_{t-1}; \mu_\theta(\mathbf{x}_t, t), \sigma_t^2 \mathbf{I})$. A forward Markov Chain is also constructed as $q(\mathbf{x}_{1:T}|\mathbf{x}_0) = \prod_{t=1}^T q(\mathbf{x}_t|\mathbf{x}_{t-1})$, allowing $\mu_\theta(\mathbf{x}_t, t)$ to be defined as: $\frac{1}{\sqrt{\alpha_t}} \left(\mathbf{x}_t - \frac{\beta_t}{\sqrt{1-\alpha_t}} \epsilon_\theta(\mathbf{x}_t, t) \right)$, where the noise predictor ϵ_θ is trained using the loss function:

$$\ell = \mathbb{E}_{t, \mathbf{x}_0, \epsilon} [\|\epsilon - \epsilon_\theta(\sqrt{\alpha_t} \mathbf{x}_0 + \sqrt{1-\alpha_t} \epsilon, t)\|_2], \quad (1)$$

with $\bar{\alpha}_t$ as a constant and ϵ sampled from a standard normal distribution. Building on the foundation of diffusion models, latent diffusion models [53] extend this approach by mapping data into a low-dimensional latent space using a pre-trained variational auto-encoder (VAE) [12]. The diffusion process is then applied within this latent space, which significantly reduces computational costs and allows these models to handle larger datasets and more complex tasks, such as video and 3D generation. In our work, we fine-tune our diffusion models using these advanced latent diffusion models and their variants to achieve our specific goals.

3.2. Problem Formulation

Given a human image X and a sequence of driving poses $p_{1:T}$, we aim to generate a human animation video $Y_{1:T}$. We propose to capture the correlations in a coarse-to-fine manner, facilitating both intra-frame coherence and inter-frame consistency. Specifically, we first jointly generate fine-grained image x_t , depth d_t , and normal maps n_t in low-resolution space to enrich guidance for each frame t with a Mutually Aligned Geometry Diffusion Model G_1 . Then we incorporate multiple guidance to animate the human image utilizing a high-resolution Cross-domain Controlled Video Diffusion Model G_2 with a cross-domain controller. Note that we drop the low-resolution RGB images $x_{1:T}$ generated in the first stage. The overall pipeline can be formulated as,

$$\begin{aligned} x_{1:T}, n_{1:T}, d_{1:T} &= G_1^{low-res}(X, p_{1:T}) \\ Y_{1:T} &= G_2^{high-res}(X, p_{1:T}, n_{1:T}, d_{1:T}) \end{aligned} \quad (2)$$

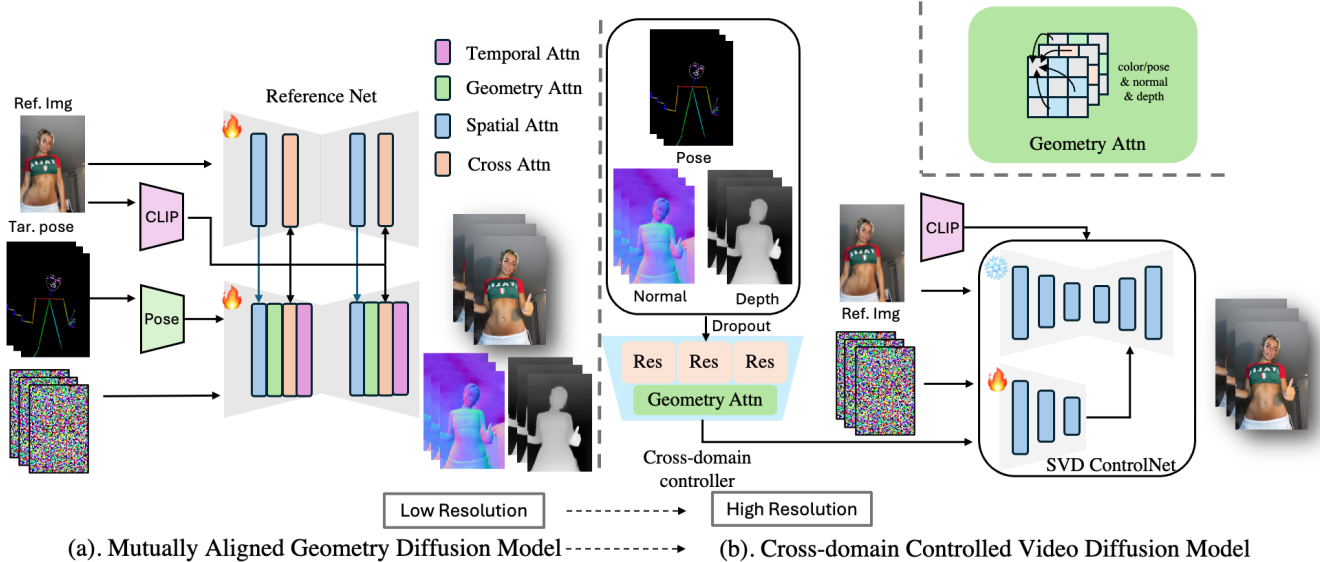


Figure 2. **Overview of DreamDance framework.** The Mutually Aligned Geometry Diffusion Model generates detailed depth and normal maps to enrich guidance signals that are mutually aligned across modalities and time. The Cross-domain Controlled Video Diffusion Model utilizes a cross-domain controller to integrate multiple levels of guidance, producing high-quality human animations.

4. Method: DreamDance

We propose DreamDance, a unified framework for animating human images with high quality and precise control. As shown in Figure 2, our method consists of two stages according to our problem formulation in Section 3.2. Given the reference image and target poses, the Mutually Aligned Geometry Diffusion Model generates the target normal and depth maps as well as RGB images in the first stage, enriching geometry cues as guidance. Subsequently, the Cross-Domain Controlled Video Diffusion Model utilizes a cross-domain controller to integrate multiple levels of guidance for high-quality human image animating.

4.1. Mutually Aligned Geometry Diffusion Model

To enrich geometric information from the reference image given the target poses, we aim to first establish correlations that transition from a coarse-level pose skeleton to fine-grained spatial geometry. However, several challenges arise. 1). The original diffusion model is trained on RGB images, which differ significantly from geometry representations, making it difficult to model these disparate modalities within a unified diffusion process. 2). While the target pose provides the basic human structure, it lacks detailed geometry and appearance information that should be sourced from the reference image. 3). Ground truth RGB images are inherently aligned with their geometric features, necessitating the preservation of this alignment throughout the generation process to ensure coherence and accuracy.

Modeling a Unified Diffusion Process. As shown in Figure 2 (a), we model a unified diffusion process that jointly generates depth \mathbf{d} and normal maps \mathbf{n} , along with RGB im-

ages \mathbf{x} , all aligned with the target poses \mathbf{p} based on the reference images \mathbf{i} . The unified diffusion model can be trained with a simplified objective:

$$\begin{aligned} \ell &= \mathbb{E}_{t, \mathbf{z}, \mathbf{i}, \mathbf{p}, \epsilon} [\|\epsilon - \epsilon_\theta(\mathbf{z}_t; \mathbf{i}, \mathbf{p})\|_2^2] \\ \mathbf{z}_t &= \text{concat}(\mathbf{x}_t, \mathbf{n}_t, \mathbf{d}_t) \end{aligned} \quad (3)$$

where $\epsilon \sim \mathcal{N}(0, I)$ are independent Gaussian noise and t is the sampled timestep that determines the scale of added noise. The noisy latents are obtained by $\mathbf{x}_t/\mathbf{n}_t/\mathbf{d}_t = \alpha_t(\mathbf{x}/\mathbf{n}/\mathbf{d}) + \sigma_t\epsilon$ and are concatenated along the batch dimension as a unified noisy latent \mathbf{z}_t , which is sent into the denoising UNet to predict the added noise. Given that the original diffusion model has a strong prior in the image domain, which differs from the distribution of depth and normal maps, we introduce a domain embedding to the UNet architecture. This aims to simplify the training process by better accommodating the distinct characteristics of each domain. Specifically, we use a one-hot vector to specify the domain of each sample, which is then encoded using positional encoding. The resulting domain embedding is added to the time embedding in the UNet. We find that incorporating the domain embedding leads to more stable training and faster convergence.

Control with Reference Image and Target Pose. Inspired by [29], we introduce a reference UNet for detailed reference image feature guidance. The spatial attention in the denoising UNet is modified as,

$$\begin{aligned} \mathbf{q} &= W_q \cdot \mathbf{x}, \\ \mathbf{k} &= W_k \cdot \text{concat}(\mathbf{x}, \mathbf{x}_{\text{ref}}), \\ \mathbf{v} &= W_v \cdot \text{concat}(\mathbf{x}, \mathbf{x}_{\text{ref}}), \end{aligned} \quad (4)$$

where \mathbf{x} is the noisy features and \mathbf{x}_{ref} is the detailed injection features from the reference UNet. These features

are concatenated along the sequence dimension. Additionally, to guide the diffusion model with the target pose, we employ a lightweight convolutional pose encoder with zero convolution projection to encode the pose embedding following [29, 96]. The pose embedding is added to the noisy latent features after the conv_in layer of the UNet.

Mutual Alignment with Geometry Attention. We now extend the original diffusion model to jointly generate normal and depth maps, along with RGB images, all semantically aligned with the target pose and reference image. However, there is no inherent guarantee that these generated outputs will be mutually consistent. To address this, we propose a geometry attention module that aligns the geometric representations and RGB images during the diffusion process, ensuring coherence across the generated content. The geometry attention is modified based on the self-attention mechanism in which the queries, keys, and values for each different modality are computed as follows,

$$\begin{aligned} \mathbf{q}_i &= W_q \cdot \mathbf{x}_i, & \mathbf{q}_n &= W_q \cdot \mathbf{x}_n, & \mathbf{q}_d &= W_q \cdot \mathbf{x}_d, \\ \mathbf{k}_i &= W_k \cdot \text{cat}(\mathbf{x}_i, \mathbf{x}_n, \mathbf{x}_d), & \mathbf{v}_i &= W_v \cdot \text{cat}(\mathbf{x}_i, \mathbf{x}_n, \mathbf{x}_d), \\ \mathbf{k}_n &= W_k \cdot \text{cat}(\mathbf{x}_i, \mathbf{x}_n, \mathbf{x}_d), & \mathbf{v}_n &= W_v \cdot \text{cat}(\mathbf{x}_i, \mathbf{x}_n, \mathbf{x}_d), \\ \mathbf{k}_d &= W_k \cdot \text{cat}(\mathbf{x}_i, \mathbf{x}_n, \mathbf{x}_d), & \mathbf{v}_d &= W_v \cdot \text{cat}(\mathbf{x}_i, \mathbf{x}_n, \mathbf{x}_d), \end{aligned} \quad (5)$$

where $\text{cat}()$ refers to the concatenation operation along the sequence dimension. The geometry attention module enhances mutual-guided geometric consistency, ensuring the generated geometric information remains stable and reliable. Additionally, we incorporate a temporal attention module to smooth the generated content, promoting temporal consistency. By aligning geometric information across both modality and temporal dimensions, we establish a robust foundation for effective control in the subsequent stages of video generation.

Training Strategy. The training process is conducted in three steps. First, we disable the geometry and temporal attention to train the model using random inputs from different modalities. This allows the model to learn independently from each modality without the complexity of cross-modal and temporal interactions. Next, the geometry attention is activated with the other modules freeze, focusing on aligning the different modalities. Finally, we activate the temporal attention and freeze the other modules, ensuring temporal consistency. This three-step strategy stabilizes the training process by gradually introducing the complexity of multi-modal alignment and temporal consistency, ensuring stable convergence. At this stage, all the training steps are conducted at a relatively low resolution to balance efficiency and performance effectively. We empirically find this strategy can not only stabilize the process and accelerate convergence but also result in minimal performance loss compared to training at high resolution.

Multi-domain CFG. Classifier-free guidance [24] (CFG) is a technique that enables a balance between sample quality

and diversity for diffusion models. Our empirical observations indicate that different domains generated by our diffusion model require distinct optimal guidance scales for best results, especially for normal maps. Thus we propose multi-domain CFG(MCFG) to apply different guidance scales to each domain based on Equation 3 and formulate as follows,

$$\begin{aligned} \epsilon_\theta(\mathbf{x}_t; \mathbf{i}, \mathbf{p}), \epsilon_\theta(\mathbf{n}_t; \mathbf{i}, \mathbf{p}), \epsilon_\theta(\mathbf{d}_t; \mathbf{i}, \mathbf{p}) &= \text{chunk}(\epsilon_\theta(\mathbf{z}_t; \mathbf{i}, \mathbf{p})) \\ \tilde{\epsilon}_\theta(\mathbf{x}_t; \mathbf{i}, \mathbf{p}) &= \epsilon_\theta(\mathbf{x}_t; \mathbf{i}, \mathbf{p}) + s_x \cdot (\epsilon_\theta(\mathbf{x}_t; \mathbf{i}, \mathbf{p}) - \epsilon_\theta(\mathbf{x}_t; \emptyset, \mathbf{p})) \\ \tilde{\epsilon}_\theta(\mathbf{n}_t; \mathbf{i}, \mathbf{p}) &= \epsilon_\theta(\mathbf{n}_t; \mathbf{i}, \mathbf{p}) + s_n \cdot (\epsilon_\theta(\mathbf{n}_t; \mathbf{i}, \mathbf{p}) - \epsilon_\theta(\mathbf{n}_t; \emptyset, \mathbf{p})) \\ \tilde{\epsilon}_\theta(\mathbf{d}_t; \mathbf{i}, \mathbf{p}) &= \epsilon_\theta(\mathbf{d}_t; \mathbf{i}, \mathbf{p}) + s_d \cdot (\epsilon_\theta(\mathbf{d}_t; \mathbf{i}, \mathbf{p}) - \epsilon_\theta(\mathbf{d}_t; \emptyset, \mathbf{p})) \end{aligned} \quad (6)$$

4.2. Cross-domain Controlled Video Diffusion Model

With the enriched guidance signals (i.e., depth and normal maps) mutually consistent and aligned with the target pose, we now aim to integrate these various types of guidance into a video diffusion model to animate human images. Note that we drop the low-resolution RGB images generated in the previous stage.

Cross-domain Controller As shown in Figure 2 (b.), We introduce a cross-domain controller to integrate multiple guidance signals, enabling high-fidelity and accurate animation of human images. Specifically, each control signal modality—such as depth, normal maps, and pose, is first embedded into the feature space through a series of lightweight, domain-specific convolutional layers. This step captures the essential features of each modality. Next, we employ a similar geometry attention mechanism, as outlined in Equation 5, to integrate these feature vectors, ensuring harmonious interaction across modalities. This unified guidance feature drives the animation process with coherence and precision. Formally, the guidance feature \mathbf{f} for each frame is obtained by

$$\mathbf{f}_i = \text{GeoAttn}(F_p(\mathbf{p}_i), F_d(\mathbf{d}_i), F_n(\mathbf{n}_i)), i \in [0 : T] \quad (7)$$

where F_p, F_d, F_n are the domain-specific convolution encoders. The guidance feature is then added to the noisy latent features after the conv_in layer of the SVD ControlNet. **SVD ControlNet.** To effectively control the video diffusion model generation process, we adapt the ControlNet [92] on the SVD model. Specifically, SVD ControlNet freezes all parameters of the pre-trained SVD, while keeping a trainable copy of selected layers from the original network. These two branches are linked by zero-initialized convolution layers that gradually incorporate controllable features during training. Empirically, we find that using SVD ControlNet leads to more stable training compared to fine-tuning the entire network.

Robust Conditioning. Since the generated depth and normal conditions from the first stage may contain artifacts, error accumulation becomes a potential issue in our two-stage pipeline, potentially leading to performance degra-

Method	Original Guidance	Image				Video	
		L1↓	PSNR↑	SSIM↑	LPIPS↓	FID-VID↓	FVD↓
MRAA [58]	2D	3.21E-04	29.39	0.672	0.296	54.47	284.82
DisCo [68]	2D	3.78E-04	29.03	0.668	0.292	59.90	292.80
AnimateAnyone [29]	2D	-	29.56	0.718	0.285	-	171.90
MagicAnimate [79]	2D	3.13E-04	29.16	0.714	0.239	<u>21.75</u>	179.07
Champ [96]	2D+3D	<u>3.02E-04</u>	<u>29.84</u>	<u>0.773</u>	<u>0.235</u>	26.14	<u>170.20</u>
Ours	2D	2.89E-04	29.90	0.798	0.233	19.86	153.07

(a) Quantitative comparisons on TikTok dataset.

Method	Original Guidance	Image				Video	
		L1↓	PSNR↑	SSIM↑	LPIPS↓	FID-VID↓	FVD↓
AnimateAnyone [29]	2D	3.25E-04	29.37	0.725	0.278	<u>22.69</u>	<u>177.38</u>
MagicAnimate [79]	2D	3.47E-04	29.09	0.712	0.291	28.23	196.77
Champ [96]	2D+3D	<u>3.19E-04</u>	<u>29.60</u>	<u>0.746</u>	<u>0.243</u>	23.83	182.25
Ours	2D	2.83E-04	29.85	0.788	0.233	20.37	158.24

(b) Quantitative comparisons on the proposed dataset.

Table 1. Quantitative comparisons with baselines, with best results in **bold** and second best results underlined.

dation. To mitigate this, we propose a simple yet effective dropout strategy for the control signals to enhance robust conditioning. Specifically, we randomly replace control signals across temporal dimensions and modalities with zero-value images, encouraging the model to leverage cues from alternative modalities and temporal frames rather than strictly adhering to the conditions. This approach significantly improves robustness during inference and proves especially effective in enhancing temporal consistency.

5. Experiments

5.1. TikTok-Dance5K Dataset

Large-scale datasets with high-quality samples are important for video generation tasks. We construct a human dance dataset consisting of around 5K videos to facilitate high-fidelity human image animation. All the samples are collected from TikTok and followed by a manual cleaning process. We preprocess the dataset to obtain pseudo ground truth pose, normal, and depth maps [2, 81, 82]. The dataset will be made publicly available.

5.2. Implementation Details

Our experiments are conducted on 8 NVIDIA A800 GPUs. To train the geometry diffusion model in the first stage, we initialize both the reference UNet and denoising UNet with Stable Diffusion v1.5. The training resolution is 256x384. As for the video diffusion model in the second stage, we initialize the model with SVD v1.1 and train the model for 50,000 steps with a batch size of 8. The training video is cropped and resized to the resolution of 512x768 and comprises 16 frames. For more details on the training settings, please refer to the Appendix.

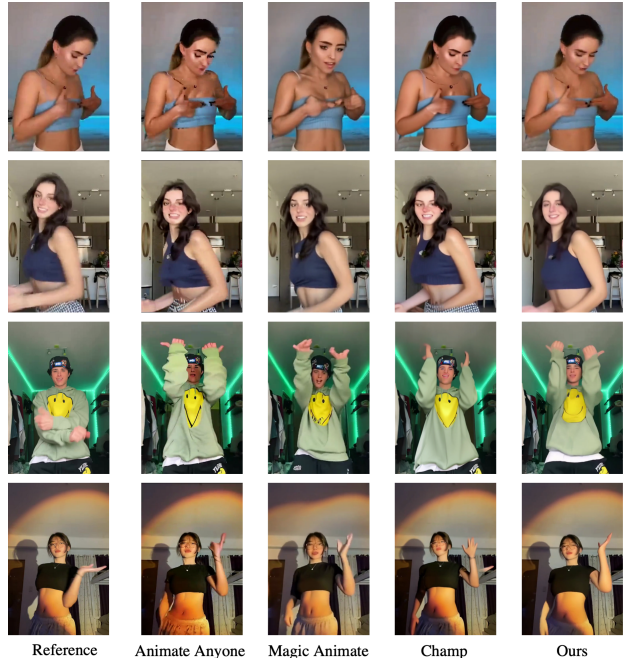


Figure 3. Qualitative results comparing to baseline methods. The first two rows are from the TikTok dataset and the last two are from the proposed dataset’s testing set.

5.3. Main Results

Baselines. MRAA [58] is the state-of-the-art GAN-based animation method that warps the source image by estimating the optical flow of the driving sequence and then inpaints the occluded regions using a GAN model. DisCo [68] is a baseline diffusion-based animation method that integrates a module of separation conditions for pose, body, and background into a pre-trained diffusion model for human image animation. MagicAnimate [79] and Ani-

mateAnyone [29] are diffusion-based human image animating methods that employ 2D control signals as guidance. Champ [96] is developed based on AnimateAnyone and develops a 3D representation such as SMPL to model the control sequence. The SMPL representation is rendered into depth and normal maps as well as semantic maps. Then combined with 2D skeleton poses, multiple control signals are fused and together guide the animating process.

Evaluation Metrics. Following the evaluation method in previous works, we adopt L1 error, Structural Similarity Index (SSIM) [73], Learned Perceptual Image Patch Similarity (LPIPS) [93], and Peak Signal-to-Noise Ratio (PSNR) [28] to evaluate single-frame image quality. To evaluate video fidelity, we use Fréchet Inception Distance with Fréchet Video Distance (FID-FVD) [3] and Fréchet Video Distance (FVD) [65].

Evaluation on the Benchmark Dataset. We evaluate our proposed method on the benchmark dataset TikTok dataset [32] and report metrics in Table 1a. Our method shows state-of-the-art performance compared to baseline methods, achieving lower L1 losses, LPIPS, FID-VID, FVD scores, and higher PSNR, and SSIM values. We also provide qualitative results in Figure 3.



Figure 4. Qualitative results with generated normal and depth.

Evaluation on the Proposed Dataset. To further evaluate our proposed method, we conduct experiments on the testing set of our proposed dataset. We report the evaluation metrics in Table 1b and present qualitative comparisons in Figure 3. Our method achieves state-of-the-art performance compared to various baseline methods. We present more qualitative results with generated normal and depth guidance in Figure 4. We observe that both AnimateAnyone [29] and MagicAnimate [79] produce low-quality results due to insufficient guidance, while Champ [96] fail to generate accurate details, especially in the hand area. This is because SMPL struggles to reconstruct complex hand

poses, leading to imprecise guidance map renderings.

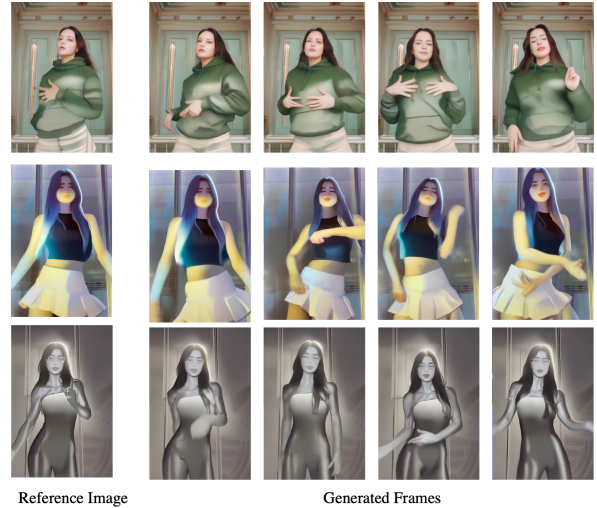


Figure 5. Qualitative results of animating unseen domain images.

Animating Unseen Domain Images. We present qualitative results of animating images from unseen domains in Figure 5, using the obtained normal and depth conditions. These results demonstrate the generalization capabilities of the proposed method.



Figure 6. Qualitative results of cross-ID animation.

Cross-ID Animation. We animate different human images with the same pose sequence and present in Figure 6.

Inference Efficiency Analysis. Table 2 presents the inference efficiency analysis of our proposed method. We report the average time consumption of obtaining all the guidance maps when only 2D pose skeletons are given. Results show that our method consumes a similar time compared to Champ [96]. Considering Champ requires multiple steps when obtaining guidance maps, including 3D prediction, 3D smoothness, shape transfer, and rendering, our method

Method	Stage 1	Total
Ours	1.13s	1.13s

Method	3D prediction & smooth	shape transfer & rendering	Total
Champ [96]	0.55s	0.43s	0.98s

Table 2. Inference efficiency analysis for obtaining geometry guidance. We report average inference time per frame in seconds.

Guidance	L1↓	PSNR↑	SSIM↑	LPIPS↓	FID-VID↓	FVD↓
a). Without Pose	3.38E-04	29.43	0.743	0.255	22.38	175.37
b). Without Depth	3.95E-04	29.02	0.701	0.277	24.56	193.23
c). Without Normal	3.67E-04	29.24	0.723	0.263	23.28	183.84
d). Pose+Normal+Depth	2.89E-04	29.90	0.798	0.233	19.86	153.07

(a) Ablation studies on different conditions.

Controller	L1↓	PSNR↑	SSIM↑	LPIPS↓	FID-VID↓	FVD↓
Without GeoAttn	3.36E-04	29.48	0.767	0.242	21.93	165.27
With GeoAttn	2.89E-04	29.90	0.798	0.233	19.86	153.07

(b) Ablation studies on the effectiveness of geometry attention.

Table 3. Quantitative ablation studies.

that generates all the guidance maps using a single diffusion model is more efficient and user-friendly.

5.4. Ablation studies

Different Conditions. We conduct comprehensive experiments on different variants of the conditions incorporated in the video diffusion model to show the effectiveness of the proposed method. As shown in Table 3a, comparing different variants a), b), c) with our method d), we show that the incorporation of multiple conditions achieves robust and best performance. Qualitative comparisons are presented in Figure 7. We observe that without depth or normal maps, the quality of the generation is noticeably flawed. Meanwhile, as originally provided, the pose maps provide refined guidance for facial and hand regions, improving generation quality.

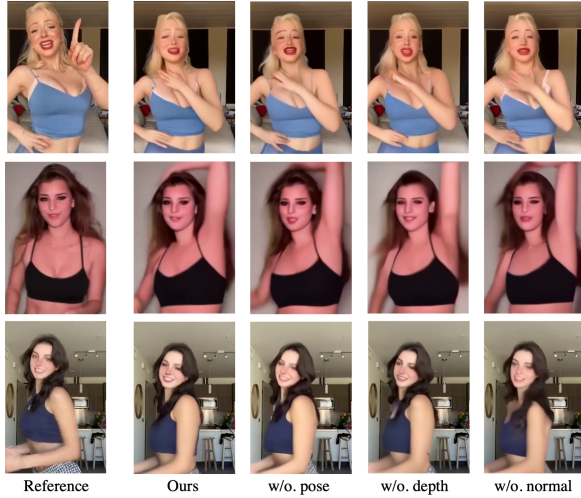


Figure 7. Qualitative ablation studies on different conditions.

Geometry Alignment. To validate the effectiveness of the proposed geometry attention and the MCFG strategy for geometry alignment in the first stage, we show qualitative ablation studies in Figure 9. Without MCFG, the generated normal maps show an over-saturated color that cannot represent normal information effectively. Without the geometry attention, normal and depth maps are not aligned with



Figure 8. Qualitative results of ablation studies on the effectiveness of geometry attention.

each other.

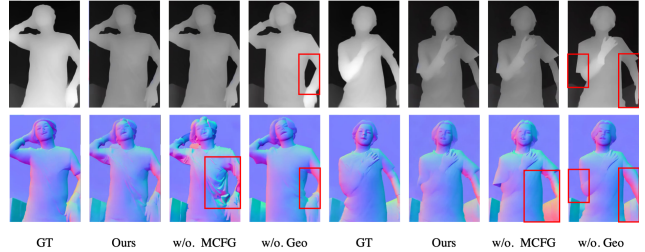


Figure 9. Qualitative ablation studies on the effectiveness of proposed modules for geometry alignment. (Please zoom in to view.)

Geometry Attention for Conditions Fusion. We conduct an ablation study to evaluate the effectiveness of the proposed geometry attention mechanism for conditions fusion. Quantitative comparisons are presented in Table 3b, demonstrating that including geometry attention significantly enhances performance. Additionally, qualitative comparisons in Figure 8 further illustrate its benefits. We observe geometry attention effectively integrates multiple types of conditions, leading to more robust and high-quality generation.

6. Conclusion

This paper introduces DreamDance, a unified framework for animating human images using skeleton pose sequences. By employing innovative two-stage diffusion models, including the Mutually Aligned Geometry Diffusion Model

to enrich guidance signals and the Cross-domain Controlled Video Diffusion Model to integrate multiple levels of guidance, DreamDance significantly enhances visual coherence and temporal consistency of the generated video. Extensive experiments demonstrate that the proposed method achieves state-of-the-art performance, offering a flexible and user-friendly solution for realistic human image animating.

References

- [1] Badour AlBahar, Shunsuke Saito, Hung-Yu Tseng, Changil Kim, Johannes Kopf, and Jia-Bin Huang. Single-image 3d human digitization with shape-guided diffusion. In *SIG-GRAPH Asia*, 2023. 3
- [2] Gwangbin Bae and Andrew J. Davison. Rethinking inductive biases for surface normal estimation. In *IEEE/CVF Conference on Computer Vision and Pattern Recognition (CVPR)*, 2024. 6
- [3] Yogesh Balaji, Martin Renqiang Min, Bing Bai, Rama Chelappa, and Hans Peter Graf. Conditional gan with discriminative filter generation for text-to-video synthesis. In *IJCAI*, page 2, 2019. 7
- [4] Andreas Blattmann, Tim Dockhorn, Sumith Kulal, Daniel Mendelevitch, Maciej Kilian, Dominik Lorenz, Yam Levi, Zion English, Vikram Voleti, Adam Letts, et al. Stable video diffusion: Scaling latent video diffusion models to large datasets. *arXiv preprint arXiv:2311.15127*, 2023. 1, 3
- [5] Andreas Blattmann, Robin Rombach, Huan Ling, Tim Dockhorn, Seung Wook Kim, Sanja Fidler, and Karsten Kreis. Align your latents: High-resolution video synthesis with latent diffusion models. In *Proceedings of the IEEE/CVF Conference on Computer Vision and Pattern Recognition*, pages 22563–22575, 2023. 1, 3
- [6] Tim Brooks, Aleksander Holynski, and Alexei A Efros. Instructpix2pix: Learning to follow image editing instructions. *arXiv preprint arXiv:2211.09800*, 2022. 1
- [7] Yukang Cao, Yan-Pei Cao, Kai Han, Ying Shan, and Kwan-Yee K. Wong. Dreamavatar: Text-and-shape guided 3d human avatar generation via diffusion models. In *Proceedings of the IEEE/CVF Conference on Computer Vision and Pattern Recognition*, pages 958–968, 2024. 3
- [8] Caroline Chan, Shiry Ginosar, Tinghui Zhou, and Alexei A Efros. Everybody dance now. In *IEEE International Conference on Computer Vision (ICCV)*, 2019. 3
- [9] Di Chang, Yichun Shi, Quankai Gao, Jessica Fu, Hongyi Xu, Guoxian Song, Qing Yan, Xiao Yang, and Mohammad Soleymani. Magicedance: Realistic human dance video generation with motions & facial expressions transfer. *arXiv preprint arXiv:2311.12052*, 2023. 3
- [10] Haoxin Chen, Yong Zhang, Xiaodong Cun, Menghan Xia, Xintao Wang, Chao Weng, and Ying Shan. Videocrafter2: Overcoming data limitations for high-quality video diffusion models. In *Proceedings of the IEEE/CVF Conference on Computer Vision and Pattern Recognition*, pages 7310–7320, 2024. 3
- [11] Zijun Chen, Yu Wang, Liuzhenghao Lv, Hao Li, Zongying Lin, Li Yuan, and Yonghong Tian. Multi-granularity score-based generative framework enables efficient inverse design of complex organics. *arXiv preprint arXiv:2409.07912*, 2024. 3
- [12] Patrick Esser, Robin Rombach, and Bjorn Ommer. Taming transformers for high-resolution image synthesis. In *Proceedings of the IEEE/CVF conference on computer vision and pattern recognition*, pages 12873–12883, 2021. 3
- [13] Patrick Esser, Johnathan Chiu, Parmida Atighehchian, Jonathan Granskog, and Anastasis Germanidis. Structure and content-guided video synthesis with diffusion models. In *Proceedings of the IEEE/CVF International Conference on Computer Vision*, pages 7346–7356, 2023. 3
- [14] Zixun Fang, Wei Zhai, Aimin Su, Hongliang Song, Kai Zhu, Mao Wang, Yu Chen, Zhiheng Liu, Yang Cao, and Zheng-Jun Zha. Vivid: Video virtual try-on using diffusion models. *arXiv preprint arXiv:2405.11794*, 2024. 3
- [15] Mengyang Feng, Jinlin Liu, Kai Yu, Yuan Yao, Zheng Hui, Xiefan Guo, Xianhui Lin, Haolan Xue, Chen Shi, Xiaowen Li, et al. Dreamoving: A human dance video generation framework based on diffusion models. *arXiv preprint arXiv:2312.05107*, 2023. 3
- [16] Xiao Fu, Wei Yin, Mu Hu, Kaixuan Wang, Yuexin Ma, Ping Tan, Shaojie Shen, Dahua Lin, and Xiaoxiao Long. Geowizard: Unleashing the diffusion priors for 3d geometry estimation from a single image. In *ECCV*, 2024. 2
- [17] Scott Geng, Revant Teotia, Purva Tendulkar, Sachit Menon, and Carl Vondrick. Affective faces for goal-driven dyadic communication. *arXiv preprint arXiv:2301.10939*, 2023. 3
- [18] Michal Geyer, Omer Bar-Tal, Shai Bagon, and Tali Dekel. Tokenflow: Consistent diffusion features for consistent video editing. *arXiv preprint arXiv:2307.10373*, 2023. 3
- [19] Jianzhu Guo, Dingyun Zhang, Xiaoqiang Liu, Zhizhou Zhong, Yuan Zhang, Pengfei Wan, and Di Zhang. Liveportrait: Efficient portrait animation with stitching and retargeting control. *arXiv preprint arXiv:2407.03168*, 2024. 3
- [20] Xun Guo, Mingwu Zheng, Liang Hou, Yuan Gao, Yufan Deng, Pengfei Wan, Di Zhang, Yufan Liu, Weiming Hu, Zhengjun Zha, et al. I2v-adapter: A general image-to-video adapter for diffusion models. In *ACM SIGGRAPH 2024 Conference Papers*, pages 1–12, 2024. 3
- [21] Yuwei Guo, Ceyuan Yang, Anyi Rao, Zhengyang Liang, Yaohui Wang, Yu Qiao, Maneesh Agrawala, Dahua Lin, and Bo Dai. Animatediff: Animate your personalized text-to-image diffusion models without specific tuning. *arXiv preprint arXiv:2307.04725*, 2023. 3
- [22] Xuanhua He, Quande Liu, Shengju Qian, Xin Wang, Tao Hu, Ke Cao, Keyu Yan, and Jie Zhang. Id-animator: Zero-shot identity-preserving human video generation. *arXiv preprint arXiv:2404.15275*, 2024. 3
- [23] Zijian He, Peixin Chen, Guangrun Wang, Guanbin Li, Philip HS Torr, and Liang Lin. Wildvidfit: Video virtual try-on in the wild via image-based controlled diffusion models. *arXiv preprint arXiv:2407.10625*, 2024. 3
- [24] Jonathan Ho and Tim Salimans. Classifier-free diffusion guidance. *arXiv preprint arXiv:2207.12598*, 2022. 5
- [25] Jonathan Ho, Ajay Jain, and Pieter Abbeel. Denoising diffusion probabilistic models. *Advances in Neural Information Processing Systems*, 33:6840–6851, 2020. 1, 3

- [26] Jonathan Ho, Tim Salimans, Alexey Gritsenko, William Chan, Mohammad Norouzi, and David J Fleet. Video diffusion models. *Advances in Neural Information Processing Systems*, 35:8633–8646, 2022. 3
- [27] Wenyi Hong, Ming Ding, Wendi Zheng, Xinghan Liu, and Jie Tang. Cogvideo: Large-scale pretraining for text-to-video generation via transformers. *arXiv preprint arXiv:2205.15868*, 2022. 3
- [28] Alain Hore and Djemel Ziou. Image quality metrics: Psnr vs. ssim. In *2010 20th international conference on pattern recognition*, pages 2366–2369. IEEE, 2010. 7
- [29] Li Hu. Animate anyone: Consistent and controllable image-to-video synthesis for character animation. In *Proceedings of the IEEE/CVF Conference on Computer Vision and Pattern Recognition*, pages 8153–8163, 2024. 1, 3, 4, 5, 6, 7
- [30] Ziqi Huang, Yinan He, Jiashuo Yu, Fan Zhang, Chenyang Si, Yuming Jiang, Yuanhan Zhang, Tianxing Wu, Qingyang Jin, Nattapol Chanpaisit, et al. Vbench: Comprehensive benchmark suite for video generative models. In *Proceedings of the IEEE/CVF Conference on Computer Vision and Pattern Recognition*, pages 21807–21818, 2024. 3
- [31] Ziyao Huang, Fan Tang, Yong Zhang, Xiaodong Cun, Juan Cao, Jintao Li, and Tong-Yee Lee. Make-your-anchor: A diffusion-based 2d avatar generation framework. In *Proceedings of the IEEE/CVF Conference on Computer Vision and Pattern Recognition*, pages 6997–7006, 2024. 3
- [32] Yasamin Jafarian and Hyun Soo Park. Learning high fidelity depths of dressed humans by watching social media dance videos. In *Proceedings of the IEEE/CVF Conference on Computer Vision and Pattern Recognition (CVPR)*, pages 12753–12762, 2021. 7
- [33] Jianwen Jiang, Gaojie Lin, Zhengkun Rong, Chao Liang, Yongming Zhu, Jiaqi Yang, and Tianyun Zhong. Mobile-portrait: Real-time one-shot neural head avatars on mobile devices. *arXiv preprint arXiv:2407.05712*, 2024. 3
- [34] Peng Jin, Yang Wu, Yanbo Fan, Zhongqian Sun, Yang Wei, and Li Yuan. Act as you wish: Fine-grained control of motion diffusion model with hierarchical semantic graphs. In *NeurIPS*, 2023. 3
- [35] Peng Jin, Hao Li, Zesen Cheng, Kehan Li, Runyi Yu, Chang Liu, Xiangyang Ji, Li Yuan, and Jie Chen. Local action-guided motion diffusion model for text-to-motion generation. In *European Conference on Computer Vision*, pages 392–409. Springer, 2024. 3
- [36] Johanna Karras, Aleksander Holynski, Ting-Chun Wang, and Ira Kemelmacher-Shlizerman. Dreampose: Fashion image-to-video synthesis via stable diffusion. In *2023 IEEE/CVF International Conference on Computer Vision (ICCV)*, pages 22623–22633. IEEE, 2023. 1, 3
- [37] Bingxin Ke, Anton Obukhov, Shengyu Huang, Nando Metzger, Rodrigo Caye Daudt, and Konrad Schindler. Repurposing diffusion-based image generators for monocular depth estimation. In *Proceedings of the IEEE/CVF Conference on Computer Vision and Pattern Recognition (CVPR)*, 2024. 2
- [38] Levon Khachatryan, Andranik Movsisyan, Vahram Tadevosyan, Roberto Henschel, Zhangyang Wang, Shant Navasardyan, and Humphrey Shi. Text2video-zero: Text-to-image diffusion models are zero-shot video generators. In *Proceedings of the IEEE/CVF International Conference on Computer Vision*, pages 15954–15964, 2023. 3
- [39] Jeongho Kim, Min-Jung Kim, Junsoo Lee, and Jaegul Choo. Tcan: Animating human images with temporally consistent pose guidance using diffusion models. *arXiv preprint arXiv:2407.09012*, 2024. 3
- [40] Xian Liu, Jian Ren, Aliaksandr Siarohin, Ivan Skorokhodov, Yanyu Li, Dahua Lin, Xihui Liu, Ziwei Liu, and Sergey Tulyakov. Hyperhuman: Hyper-realistic human generation with latent structural diffusion. *arXiv preprint arXiv:2310.08579*, 2023. 2
- [41] Xiaoxiao Long, Yuan-Chen Guo, Cheng Lin, Yuan Liu, Zhiyang Dou, Lingjie Liu, Yuexin Ma, Song-Hai Zhang, Marc Habermann, Christian Theobalt, et al. Wonder3d: Single image to 3d using cross-domain diffusion. *arXiv preprint arXiv:2310.15008*, 2023. 2
- [42] Matthew Loper, Naureen Mahmood, Javier Romero, Gerard Pons-Moll, and Michael J Black. Smpl: A skinned multi-person linear model. In *Seminal Graphics Papers: Pushing the Boundaries, Volume 2*, pages 851–866. 2023. 2
- [43] Yue Ma, Hongyu Liu, Hongfa Wang, Heng Pan, Yingqing He, Junkun Yuan, Ailing Zeng, Chengfei Cai, Heung-Yeung Shum, Wei Liu, et al. Follow-your-emoji: Fine-controllable and expressive freestyle portrait animation. *arXiv preprint arXiv:2406.01900*, 2024. 3
- [44] Yifang Men, Yuan Yao, Miaomiao Cui, and Liefeng Bo. Mimo: Controllable character video synthesis with spatial decomposed modeling. *arXiv preprint arXiv:2409.16160*, 2024. 3
- [45] Chong Mou, Xintao Wang, Liangbin Xie, Yanze Wu, Jian Zhang, Zhongang Qi, and Ying Shan. T2i-adapter: Learning adapters to dig out more controllable ability for text-to-image diffusion models. In *Proceedings of the AAAI Conference on Artificial Intelligence*, pages 4296–4304, 2024. 2
- [46] nonnonstop. sd-webui-3d-open-pose-editor. <https://github.com/nonnonstop/sd-webui-3d-open-pose-editor>, 2024. Accessed: 2024-07-13. 2
- [47] Yatian Pang, Tanghui Jia, Yujun Shi, Zhenyu Tang, Junwu Zhang, Xinhua Cheng, Xing Zhou, Francis E. H. Tay, and Li Yuan. Envision3d: One image to 3d with anchor views interpolation, 2024. 2, 3
- [48] William Peebles and Saining Xie. Scalable diffusion models with transformers. *arXiv preprint arXiv:2212.09748*, 2022. 1
- [49] Bohao Peng, Jian Wang, Yuechen Zhang, Wenbo Li, Ming-Chang Yang, and Jiaya Jia. Controlnext: Powerful and efficient control for image and video generation. *arXiv preprint arXiv:2408.06070*, 2024. 3
- [50] Chenyang Qi, Xiaodong Cun, Yong Zhang, Chenyang Lei, Xintao Wang, Ying Shan, and Qifeng Chen. Fatezero: Fusing attentions for zero-shot text-based video editing. In *Proceedings of the IEEE/CVF International Conference on Computer Vision*, pages 15932–15942, 2023. 3
- [51] Lingteng Qiu, Guanying Chen, Xiaodong Gu, Qi Zuo, Mutian Xu, Yushuang Wu, Weihao Yuan, Zilong Dong, Liefeng Bo, and Xiaoguang Han. Richdreamer: A generalizable normal-depth diffusion model for detail richness in text-to-

- 3d. In *Proceedings of the IEEE/CVF Conference on Computer Vision and Pattern Recognition*, pages 9914–9925, 2024. 2
- [52] Yurui Ren, Ge Li, Shan Liu, and Thomas H Li. Deep spatial transformation for pose-guided person image generation and animation. *IEEE Transactions on Image Processing*, 2020. 3
- [53] Robin Rombach, Andreas Blattmann, Dominik Lorenz, Patrick Esser, and Björn Ommer. High-resolution image synthesis with latent diffusion models. In *Proceedings of the IEEE/CVF Conference on Computer Vision and Pattern Recognition*, pages 10684–10695, 2022. 1, 2, 3
- [54] Nataniel Ruiz, Yuanzhen Li, Varun Jampani, Yael Pritch, Michael Rubinstein, and Kfir Aberman. Dreambooth: Fine tuning text-to-image diffusion models for subject-driven generation. *arXiv preprint arxiv:2208.12242*, 2022. 1
- [55] Ruizhi Shao, Youxin Pang, Zerong Zheng, Jingxiang Sun, and Yebin Liu. Human4dit: 360-degree human video generation with 4d diffusion transformer. *ACM Transactions on Graphics (TOG)*, 43(6), 2024. 3
- [56] Fengyuan Shi, Jiayi Gu, Hang Xu, Songcen Xu, Wei Zhang, and Limin Wang. Bivdiff: A training-free framework for general-purpose video synthesis via bridging image and video diffusion models. In *Proceedings of the IEEE/CVF Conference on Computer Vision and Pattern Recognition*, pages 7393–7402, 2024. 3
- [57] Yujun Shi, Jun Hao Liew, Hanshu Yan, Vincent YF Tan, and Jiashi Feng. Instadrag: Lightning fast and accurate drag-based image editing emerging from videos. *arXiv preprint arXiv:2405.13722*, 2024. 2
- [58] Aliaksandr Siarohin, Oliver J Woodford, Jian Ren, Menglei Chai, and Sergey Tulyakov. Motion representations for articulated animation. In *Proceedings of the IEEE/CVF Conference on Computer Vision and Pattern Recognition*, pages 13653–13662, 2021. 6
- [59] Uriel Singer, Adam Polyak, Thomas Hayes, Xi Yin, Jie An, Songyang Zhang, Qiyuan Hu, Harry Yang, Oron Ashual, Oran Gafni, et al. Make-a-video: Text-to-video generation without text-video data. *arXiv preprint arXiv:2209.14792*, 2022. 3
- [60] Jascha Sohl-Dickstein, Eric Weiss, Niru Maheswaranathan, and Surya Ganguli. Deep unsupervised learning using nonequilibrium thermodynamics. In *International Conference on Machine Learning*, pages 2256–2265. PMLR, 2015. 3
- [61] Jiaming Song, Chenlin Meng, and Stefano Ermon. Denoising diffusion implicit models. In *Proceedings of the International Conference on Learning Representations (ICLR)*, 2021. 1
- [62] Zhenyu Tang, Junwu Zhang, Xinhua Cheng, Wangbo Yu, Chaoran Feng, Yatian Pang, Bin Lin, and Li Yuan. Cycle3d: High-quality and consistent image-to-3d generation via generation-reconstruction cycle. *arXiv preprint arXiv:2407.19548*, 2024. 3
- [63] Linrui Tian, Qi Wang, Bang Zhang, and Liefeng Bo. Emo: Emote portrait alive-generating expressive portrait videos with audio2video diffusion model under weak conditions. *arXiv preprint arXiv:2402.17485*, 2024. 3
- [64] Shuyuan Tu, Qi Dai, Zihao Zhang, Sicheng Xie, Zhi-Qi Cheng, Chong Luo, Xintong Han, Zuxuan Wu, and Yu-Gang Jiang. Motionfollower: Editing video motion via lightweight score-guided diffusion. *arXiv preprint arXiv:2405.20325*, 2024. 3
- [65] Thomas Unterthiner, Sjoerd Van Steenkiste, Karol Kurach, Raphael Marinier, Marcin Michalski, and Sylvain Gelly. Towards accurate generative models of video: A new metric & challenges. *arXiv preprint arXiv:1812.01717*, 2018. 7
- [66] Duomin Wang, Bin Dai, Yu Deng, and Baoyuan Wang. Agentavatar: Disentangling planning, driving and rendering for photorealistic avatar agents. *arXiv preprint arXiv:2311.17465*, 2023. 3
- [67] Qilin Wang, Zhengkai Jiang, Chengming Xu, Jiangning Zhang, Yabiao Wang, Xinyi Zhang, Yun Cao, Weijian Cao, Chengjie Wang, and Yanwei Fu. Vividpose: Advancing stable video diffusion for realistic human image animation. *arXiv preprint arXiv:2405.18156v1*, 2024. 3
- [68] Tan Wang, Linjie Li, Kevin Lin, Chung-Ching Lin, Zhengyuan Yang, Hanwang Zhang, Zicheng Liu, and Lijuan Wang. Disco: Disentangled control for referring human dance generation in real world. *arXiv e-prints*, pages arXiv-2307, 2023. 1, 3, 6
- [69] Xiang Wang, Hangjie Yuan, Shiwei Zhang, Dayou Chen, Jiniu Wang, Yingya Zhang, Yujun Shen, Deli Zhao, and Jingren Zhou. Videocomposer: Compositional video synthesis with motion controllability. *Advances in Neural Information Processing Systems*, 36, 2024. 3
- [70] Xiang Wang, Shiwei Zhang, Changxin Gao, Jiayu Wang, Xiaoqiang Zhou, Yingya Zhang, Luxin Yan, and Nong Sang. Unianimate: Taming unified video diffusion models for consistent human image animation. *arXiv preprint arXiv:2406.01188*, 2024.
- [71] Yuchi Wang, Junliang Guo, Jianhong Bai, Runyi Yu, Tianyu He, Xu Tan, Xu Sun, and Jiang Bian. Instructavatar: Text-guided emotion and motion control for avatar generation. *arXiv preprint arXiv:2405.15758*, 2024. 3
- [72] Yaohui Wang, Xin Ma, Xinyuan Chen, Cunjian Chen, Antitza Dantcheva, Bo Dai, and Yu Qiao. Leo: Generative latent image animator for human video synthesis. *International Journal of Computer Vision*, pages 1–13, 2024. 3
- [73] Zhou Wang, Alan C Bovik, Hamid R Sheikh, and Eero P Simoncelli. Image quality assessment: from error visibility to structural similarity. *IEEE transactions on image processing*, 13(4):600–612, 2004. 7
- [74] Zhenzhi Wang, Yixuan Li, Yanhong Zeng, Youqing Fang, Yuwei Guo, Wenran Liu, Jing Tan, Kai Chen, Tianfan Xue, Bo Dai, et al. Humanvid: Demystifying training data for camera-controllable human image animation. *arXiv preprint arXiv:2407.17438*, 2024. 3
- [75] Jay Zhangjie Wu, Yixiao Ge, Xintao Wang, Stan Weixian Lei, Yuchao Gu, Yufei Shi, Wynne Hsu, Ying Shan, Xiaohu Qie, and Mike Zheng Shou. Tune-a-video: One-shot tuning of image diffusion models for text-to-video generation. In *Proceedings of the IEEE/CVF International Conference on Computer Vision*, pages 7623–7633, 2023. 3
- [76] You Xie, Hongyi Xu, Guoxian Song, Chao Wang, Yichun Shi, and Linjie Luo. X-portrait: Expressive portrait anima-

- tion with hierarchical motion attention. In *ACM SIGGRAPH 2024 Conference Papers*, pages 1–11, 2024. 3
- [77] Yuhao Xu, Tao Gu, Weifeng Chen, and Chengcai Chen. Oot-diffusion: Outfitting fusion based latent diffusion for controllable virtual try-on. *arXiv preprint arXiv:2403.01779*, 2024.
- [78] Zhengze Xu, Mengting Chen, Zhao Wang, Linyu Xing, Zhonghua Zhai, Nong Sang, Jinsong Lan, Shuai Xiao, and Changxin Gao. Tunnel try-on: Excavating spatial-temporal tunnels for high-quality virtual try-on in videos. In *Proceedings of the 32nd ACM International Conference on Multimedia*, pages 3199–3208, 2024. 3
- [79] Zhongcong Xu, Jianfeng Zhang, Jun Hao Liew, Hanshu Yan, Jia-Wei Liu, Chenxu Zhang, Jiashi Feng, and Mike Zheng Shou. Magicanimate: Temporally consistent human image animation using diffusion model. In *Proceedings of the IEEE/CVF Conference on Computer Vision and Pattern Recognition*, pages 1481–1490, 2024. 1, 3, 6, 7
- [80] Jingyun Xue, Hongfa Wang, Qi Tian, Yue Ma, Andong Wang, Zhiyuan Zhao, Shaobo Min, Wenzhe Zhao, Kaihao Zhang, Heung-Yeung Shum, et al. Follow-your-pose v2: Multiple-condition guided character image animation for stable pose control. *arXiv preprint arXiv:2406.03035*, 2024. 3
- [81] Lihe Yang, Bingyi Kang, Zilong Huang, Xiaogang Xu, Jiashi Feng, and Hengshuang Zhao. Depth anything: Unleashing the power of large-scale unlabeled data. In *CVPR*, 2024. 6
- [82] Zhendong Yang, Ailing Zeng, Chun Yuan, and Yu Li. Effective whole-body pose estimation with two-stages distillation. In *Proceedings of the IEEE/CVF International Conference on Computer Vision*, pages 4210–4220, 2023. 6
- [83] Zhuoyi Yang, Jiayan Teng, Wendi Zheng, Ming Ding, Shiyu Huang, Jiazheng Xu, Yuanming Yang, Wenyi Hong, Xiaohan Zhang, Guanyu Feng, et al. Cogvideox: Text-to-video diffusion models with an expert transformer. *arXiv preprint arXiv:2408.06072*, 2024. 1
- [84] Hu Ye, Jun Zhang, Sibao Liu, Xiao Han, and Wei Yang. Ip-adapter: Text compatible image prompt adapter for text-to-image diffusion models. *arXiv preprint arXiv:2308.06721*, 2023. 2
- [85] Jiwen Yu, Xiaodong Cun, Chenyang Qi, Yong Zhang, Xintao Wang, Ying Shan, and Jian Zhang. Animatezero: Video diffusion models are zero-shot image animators. *arXiv preprint arXiv:2312.03793*, 2023. 3
- [86] Wing-Yin Yu, Lai-Man Po, Ray Cheung, Yuzhi Zhao, Yu Xue, and Kun Li. Bidirectionally deformable motion modulation for video-based human pose transfer. *arXiv preprint arXiv:2307.07754*, 2023. 3
- [87] Shenghai Yuan, Jinfa Huang, Yujun Shi, Yongqi Xu, Ruijie Zhu, Bin Lin, Xinhua Cheng, Li Yuan, and Jiebo Luo. Magictime: Time-lapse video generation models as metamorphic simulators. *arXiv preprint arXiv:2404.05014*, 2024. 3
- [88] Yan Zeng, Guoqiang Wei, Jiani Zheng, Jiabin Zou, Yang Wei, Yuchen Zhang, and Hang Li. Make pixels dance: High-dynamic video generation. In *Proceedings of the IEEE/CVF Conference on Computer Vision and Pattern Recognition*, pages 8850–8860, 2024. 1
- [89] Yuanhao Zhai, Kevin Lin, Linjie Li, Chung-Ching Lin, Jianfeng Wang, Zhengyuan Yang, David Doermann, Junsong Yuan, Zicheng Liu, and Lijuan Wang. Idol: Unified dual-modal latent diffusion for human-centric joint video-depth generation. *arXiv preprint arXiv:2407.10937*, 2024. 3
- [90] David Junhao Zhang, Jay Zhangjie Wu, Jia-Wei Liu, Rui Zhao, Lingmin Ran, Yuchao Gu, Difei Gao, and Mike Zheng Shou. Show-1: Marrying pixel and latent diffusion models for text-to-video generation. *International Journal of Computer Vision*, pages 1–15, 2024. 3
- [91] Junwu Zhang, Zhenyu Tang, Yatian Pang, Xinhua Cheng, Peng Jin, Yida Wei, Xing Zhou, Munan Ning, and Li Yuan. Repaint123: Fast and high-quality one image to 3d generation with progressive controllable repainting. In *European Conference on Computer Vision*, pages 303–320. Springer, 2025. 3
- [92] Lvmin Zhang, Anyi Rao, and Maneesh Agrawala. Adding conditional control to text-to-image diffusion models. In *Proceedings of the IEEE/CVF International Conference on Computer Vision*, pages 3836–3847, 2023. 2, 5
- [93] Richard Zhang, Phillip Isola, Alexei A Efros, Eli Shechtman, and Oliver Wang. The unreasonable effectiveness of deep features as a perceptual metric. In *Proceedings of the IEEE conference on computer vision and pattern recognition*, pages 586–595, 2018. 7
- [94] Yuang Zhang, Jiayi Gu, Li-Wen Wang, Han Wang, Junqi Cheng, Yuefeng Zhu, and Fangyuan Zou. Mimicmotion: High-quality human motion video generation with confidence-aware pose guidance. *arXiv preprint arXiv:2406.19680*, 2024. 3
- [95] Daquan Zhou, Weimin Wang, Hanshu Yan, Weiwei Lv, Yizhe Zhu, and Jiashi Feng. Magicvideo: Efficient video generation with latent diffusion models. *arXiv preprint arXiv:2211.11018*, 2022. 1
- [96] Shenhao Zhu, Junming Leo Chen, Zuoqiao Dai, Yinghui Xu, Xun Cao, Yao Yao, Hao Zhu, and Siyu Zhu. Champ: Controllable and consistent human image animation with 3d parametric guidance. *arXiv preprint arXiv:2403.14781*, 2024. 2, 3, 5, 6, 7
- [97] Lin Zongying, Li Hao, Lv Liuzhenghao, Lin Bin, Zhang Junwu, Chen Calvin Yu-Chian, Yuan Li, and Tian Yonghong. Taxdiff: Taxonomic-guided diffusion model for protein sequence generation. *arXiv preprint arXiv:2402.17156*, 2024. 3